Composites: Part B 42 (2011) 682–691

Contents lists available at ScienceDirect

Composites: Part B

journal homepage: www.elsevier.com/locate/compositesb

Hierarchical modelling of doubly curved laminated composite shells under distributed and localised loadings

G. Giunta [a,*], F. Biscani [a,b,c], S. Belouettar [a], E. Carrera [b]

[a] Centre de Recherche Public Henri Tudor, 29, av. John F. Kennedy, L-1855 Luxembourg-Kirchberg, Luxembourg
[b] Politecnico di Torino, 24, c.so Duca degli Abruzzi, 10129 Turin, Italy
[c] Institut Jean le Rond d'Alembert, UMR 7190, CNRS UNIV Paris 06, Case 162, Tour 55-65, 4, Place Jussieu, 75252 Paris, France

ARTICLE INFO

Article history:
Received 13 October 2010
Received in revised form 31 January 2011
Accepted 8 February 2011
Available online 12 February 2011

Keywords:
A. Carbon fibre
A. Layered structures
C. Analytical modelling
C. Laminate mechanics
Spherical shells

ABSTRACT

This paper presents a unified formulation for the modelling of doubly curved composite shell structures. Via this approach, higher-order, zig-zag, layer-wise and mixed theories can be easily formulated. Classical theories, such as Love's and Mindlin's models, can be obtained as particular cases. The governing differential equations of the static linear problem are derived in a compact general form, tackling the difficulties due to the higher than classical terms. These equations are solved via a Navier-type, closed form solution. Shells are subjected to distributed and localised loadings. Displacement and stress fields are investigated. Thin and moderately thick as well as shallow and deep shells are accounted for. Several stacking sequences are considered. Conclusions are drawn with respect to the accuracy of the theories for the considered loadings, lay-outs and geometrical parameters. The importance of the refined shell models for describing accurately the three-dimensional stress state is outlined. The proposed results might be useful as benchmark for the validation of new shell theories and finite elements.

1. Introduction

The capability to transmit surface loads by "membrane" stresses makes shells, under the same loadings, more rigid and economical than plates (see Timoshenko and Woinowsky-Krieger [1]). Over the last years, doubly curved shell structures made of composite laminae have gained widespread acceptance for primary structural components due to high value of strength- and stiffness-to-weight ratios. Many of nowadays applications may involve shells whose thickness is comparable to the radii of curvature. Localised loadings may be also present. In such cases, a three-dimensional (3D) stress state occurs locally or, even, globally. In these cases, classical theories, based on Love's [2,3] or Mindlin's [4] kinematic assumptions, may not yield a correct prediction of displacement and stress fields. Refined higher-order models are, therefore, required for an accurate and effective design.

Approximated 3D solutions can be obtained assuming that the ratio between the panel thickness and its middle surface radii is negligible as compared to unity. Under this hypothesis, the problem is governed by ordinary differentially equations with constant coefficients (see Bhimaraddi [5]). Wu et al. [6–9] developed a series of 3D asymptotic and refined asymptotic theories for the static and dynamic analyses of doubly curved laminated composite shells. The 3D problems were decomposed as a series of two-dimensional (2D) problems from which the governing equations of classical and first- or higher-order shear deformation shell theories are derived. The 3D solutions can, therefore, be obtained by solving these 2D governing equations order-by-order in a hierarchic and consistent manner. As far as 2D models are concerned, Grigolyuk and Kulikov [10], Kapania [11], Noor et al. [12,13] and Carrera [14] proposed literature reviews of classical and refined models for multi-layered shells. Reddy and Liu [15] investigated the statics and the free vibrations of cylindrical and spherical shells made of orthotropic layers via a cubic through-the-thickness approximation of the displacement components laying on the shell reference surface and a constant transverse displacement. Kinematic assumptions were such that stress-free mechanical boundary conditions at shell top and bottom were satisfied. Governing equations were solved through a Navier-type solution. Khdeir et al. [16] adopted a Lévi-type solution and the state-space concept for the static analysis of doubly curved shallow panels with different boundary conditions. A remarkable contribution on the determination of the analytical solutions of a variety of laminated composite plates and shells has been given over the recent decades by Chaudhuri and his colleagues [17–24], in which angle- and cross-ply laminates subjected to several boundary conditions were investigated via a double Fourier series approach.

* Corresponding author. Address: Advanced Materials and Structures Department, Centre de Recherche Public Henri Tudor, 29, avenue J.F. Kennedy, L-1855 Luxembourg Kirchberg, Luxembourg. Tel.: +352 42 59 91 479; fax: +352 42 59 91 555.
E-mail address: gaetano.giunta@tudor.lu (G. Giunta).

1359-8368/$ - see front matter © 2011 Elsevier Ltd. All rights reserved.
doi:10.1016/j.compositesb.2011.02.002

The present paper represents the extension of the work by Carrera and Giunta [25] to doubly curved shell structures made of composite materials and subjected to distributed and localised loadings. Linear static analysis is carried out via several 2D theories developed by means of Carrera's Unified Formulation (CUF), see Carrera [26]. CUF allows formulating several 2D models on the basis of the choice of the a-priori main unknowns (displacements or mixed models), the approximation level (laminate or lamina level), the through-the-thickness polynomial approximation order. Models that account for the transverse normal and shear deformability, the continuity of the transverse stress components and the zig-zag variation along the thickness of displacement and transverse normal stresses can be formulated straightforwardly. The governing equations are derived in the general case of doubly curved shells. Carrera et al. [27] applied CUF to the static analysis of isotropic plates undergoing localised loadings. A failure analysis of isotropic and orthotropic plates via CUF models was carried out in Carrera and Giunta [28,29]. CUF was adopted for the static analysis of isotropic, laminated and sandwich cylindrical shells under bi-sinusoidal loadings in Carrera [30,31], whereas localised loadings were assumed in Carrera and Giunta [25]. Results addressed in this work demonstrate that the 2D models based on CUF are capable of predicting the displacement and stress fields as accurately as desired. Presented results accounts for spherical shells. To the best of the authors' knowledge, not so many closed form solutions of composite spherical shells are present in literature. The presented results, accounting for several loading conditions, could be, therefore, noteworthy as benchmark for the validation of new theories and shell finite elements.

2. Overview of the considered shell theories

Geometry and curvilinear reference system (α,β,z) are presented in Fig. 1. Ω stands for the reference surface. R_α and R_β represent the curvature radii of Ω, h is the shell's thickness. Spatial coordinates are bounded such that $0 \leqslant \alpha \leqslant a$, $0 \leqslant \beta \leqslant b$ and $-h/2 \leqslant z \leqslant h/2$. Displacement components u_α, u_β and u_z are measured versus α-, β- and z-axis, respectively. A large variety of 2D theories can be formulated on the basis of different kinematic assumptions.

2.1. Classical theories

Classical theories (CTs), formulated in the last two centuries, were conceived to account for membrane-bending mechanics.

2.1.1. Classical lamination theory

Shells' Classical Lamination Theory (CLT) is based on Love's [2,3] kinematic assumptions: normals to the reference surface remain normal, straight and unstrained after deformation:

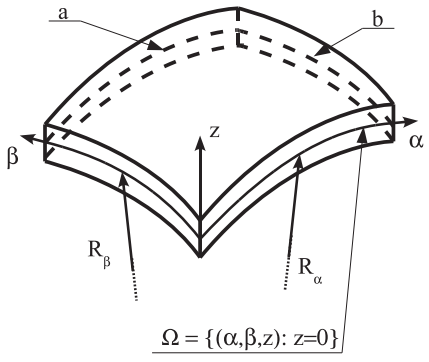

Fig. 1. Shell geometry and reference system.

$$\begin{aligned} u_q(\alpha,\beta,z) &= u_{q0}(\alpha,\beta) - z u_{z0,q} \quad q = \alpha,\beta \\ u_z(\alpha,\beta,z) &= u_{z0}(\alpha,\beta) \end{aligned} \tag{1}$$

Subscripts preceded by comma represent spatial derivation. Subscript '0' addresses model unknowns. They are the displacements in correspondence to Ω. The transverse shear and the through-the-thickness deformations are discarded. Although not adopted in this paper, a possible manner to obtain 'a-posteriori' the corresponding stresses could be the integration of the indefinite equilibrium equations, see Carrera [32]. Poisson's locking is here corrected via the assumption of reduced stiffness coefficients in Hooke's law as derived from the assumption of a plane stress state (see Carrera and Brischetto [33,34]).

2.1.2. First order shear deformation theory

Mindlin [4] postulated a kinematic field that accounts for constant transverse shear strain components along the thickness, whereas the normal deformation is neglected. Such a model is known as First Order Shear Deformation Theory (FSDT):

$$\begin{aligned} u_q(\alpha,\beta,z) &= u_{q0}(\alpha,\beta) + z u_{q1}(\alpha,\beta) \quad q = \alpha,\beta \\ u_z(\alpha,\beta,z) &= u_{z0}(\alpha,\beta) \end{aligned} \tag{2}$$

Poisson's locking is corrected via reduced stiffness coefficients. As for CLT, more accurate results could be obtained upon 'a-posteriori' integration of the indefinite equilibrium equations.

2.2. Higher-order theories

An enrichment of the displacement components u_α and u_β yields an improvement in the description of the transverse shear strain and stress components. Koiter's [35] recommendation states: "... a refinement of Love's first approximation theory is indeed meaningless, in general, unless the effects of transverse shear and normal stresses are taken into account at the same time". Transverse deformability should be also accounted for. A description of several Higher-Order Theories (HOTs) maintaining or relaxing the hypothesis of constant transverse displacement through the thickness follows.

2.2.1. HOTs including transverse normal strain

Refinements of CLT and FSDT can be introduced by enriching the displacement field of FSDT, see Eq. (2), via higher-order terms:

$$u_q(\alpha,\beta,z) = u_{q0}(\alpha,\beta) + z^r u_{qr}(\alpha,\beta) \quad q = \alpha,\beta,z \quad r = 1,2,\ldots,N \tag{3}$$

The summing convention for repeated indexes has been adopted. N is the order of expansion. Within CUF, it is a free parameter and, in this paper, it is as high as four. A N-order theory based upon Eq. (3) is addressed as 'EDN'. Letter 'E' denotes that the kinematic is preserved for the whole layers of the shell as in the so-called Equivalent Single Layer (ESL) approach. 'D' indicates that only displacement unknowns are used. 'N' stands for the expansion order of the through-the-thickness polynomial approximation. For instance, the displacement field of a ED3 model is:

$$\begin{aligned} u_\alpha &= u_{\alpha 0} + z u_{\alpha 1} + z^2 u_{\alpha 2} + z^3 u_{\alpha 3} \\ u_\beta &= u_{\beta 0} + z u_{\beta 1} + z^2 u_{\beta 2} + z^3 u_{\beta 3} \\ u_z &= u_{z0} + z u_{z1} + z^2 u_{z2} + z^3 u_{z3} \end{aligned} \tag{4}$$

This theory accounts for a parabolic and cubic variation along the thickness of transverse normal and shear strains, respectively. ED1 model experiences Poisson's locking. This is corrected assuming reduced material stiffness coefficients as done for CTs.

2.2.2. HOTs neglecting transverse normal strain

In the case transverse normal strain is discarded, the transverse displacement is considered to be constant along the thickness direction and equal to the value on the reference surface:

$$\begin{aligned} &u_q(\alpha,\beta,z) = u_{q0}(\alpha,\beta) + z^r u_{qr}(\alpha,\beta) \quad q=\alpha,\beta\ r=1,2,\ldots,N \\ &u_z(\alpha,\beta,z) = u_{z0}(\alpha,\beta) \end{aligned} \tag{5}$$

A theory of this group is denoted by 'EDND'.

2.2.3. HOTs including zig-zag effect

Laminate structures are characterised by a change in slope of displacements and transverse normal and shear stresses at layer interfaces. These quantities are C^0 class function of the transverse coordinate. EDN and EDND models are based on C^∞ functions in z and, therefore, they are intrinsically incapable to describe this zig-zag variation. This latter can be included within an ESL approach via Murakami's function $M(\zeta_k)$ (see Murakami [36] and Carrera [37]):

$$M(\zeta_k) = (-1)^k \zeta_k \tag{6}$$

where k counts the laminae and ζ_k is a local dimensionless coordinate:

$$\zeta_k = \frac{2(z-z_{0k})}{h_k} \tag{7}$$

such that $-1 \leqslant \zeta_k \leqslant 1$. h_k and z_{0k} stand for the thickness and the through-the-thickness coordinate of the mid-surface of a k-layer, respectively. The following properties hold: (a) $M(\zeta_k)$ is a piece-wise linear function of the local coordinate z_k, (b) its slope assumes opposite sign between two adjacent layers. The kinematic field including Murakami's function is:

$$\begin{aligned} &u_q(\alpha,\beta,z) = u_{q0}(\alpha,\beta) + z^r u_{qr}(\alpha,\beta) + (-1)^k \zeta_k u_{qN+1}(\alpha,\beta) \\ &q=\alpha,\beta,z \quad r=1,2,\ldots,N \end{aligned} \tag{8}$$

A model based on Murakami's function is addressed as 'EDZN'. Other possible manners of modelling the zig-zag variation are reported in Carrera [38].

2.3. Layer-wise theories

Multi-layered shells can be analysed by independent kinematic assumptions for each layer. According to Reddy [39], this approach is stated as Layer-Wise (LW). In order to satisfy the compatibility of the displacement field, a MacLaurin's expansion across the thickness, typical of ESL models, is not convenient. Interface values should be rather assumed as unknown variables. The following expansion is, therefore, adopted:

$$\begin{aligned} &u_q^k = F_t u_{qt}^k + F_b u_{qb}^k + F_r u_{qr}^k \\ &q=\alpha,\beta,z \quad r=2,3,\ldots,N \quad k=1,2,\ldots,N_l \end{aligned} \tag{9}$$

N_l represents the total number of layers. Subscripts 't' and 'b' denote values evaluated at top and bottom surface of a k-layer, respectively. The thickness functions F_t, F_b and F_r depend on ζ_k. They are defined as follows:

$$F_t = \frac{P_0+P_1}{2} \quad F_b = \frac{P_0-P_1}{2} \quad F_r = P_r - P_{r-2} \quad r=2,3,\ldots,N \tag{10}$$

$P_j = P_j(\zeta_k)$ is a Legendre's polynomials of order j. The first four Legendre's polynomials are:

$$\begin{aligned} P_0 &= 1 \quad P_1 = \zeta_k \quad P_2 = \frac{3\zeta_k^2-1}{2} \quad P_3 = \frac{5\zeta_k^3}{2} - \frac{3\zeta_k}{2} \quad P_4 \\ &= \frac{35\zeta_k^4}{8} - \frac{15\zeta_k^2}{4} + \frac{3}{8} \end{aligned} \tag{11}$$

The following properties hold:

$$\begin{aligned} &\zeta_k = 1 : F_t = 1, \quad F_b = 0, \quad F_r = 0 \\ &\zeta_k = -1 : F_t = 0, \quad F_b = 1, \quad F_r = 0 \end{aligned} \tag{12}$$

Top and bottom displacements of each lamina are assumed as unknown variable. Interlaminar compatibility of displacements can be easily linked:

$$u_{qt}^k = u_{qb}^{(k+1)} \quad q=\alpha,\beta,z \quad k=1,2,\ldots,N_l-1 \tag{13}$$

The acronym used for these theories is 'LDN', where 'L' stands for the LW approach. For all the models that have been previously described, the governing equations and the boundary conditions are derived via the Principle of Virtual Displacement (PVD).

2.4. Mixed theories based on Reissner's mixed variational theorem

The kinematics described previously does not satisfy the interlaminar continuity of transverse shear and normal stresses. It can be fulfilled 'a priori' assuming transverse shear and normal stresses together with displacements as primary variables by means of Reissner's Mixed Variational Theorem [40,41] (RMVT). Transverse stresses $\sigma_{\alpha z}^k$, $\sigma_{\beta z}^k$ and σ_{zz}^k are approximated via the same model as for the displacements (see Eq. (9)):

$$\begin{aligned} &\sigma_{qz}^k = F_t \sigma_{qzt}^k + F_b \sigma_{qzb}^k + F_r \sigma_{qzr}^k \\ &q=\alpha,\beta,z \quad r=2,3,\ldots,N \quad k=1,2,\ldots,N_l \end{aligned} \tag{14}$$

The interlaminar continuity is imposed straightforwardly:

$$\sigma_{qzt}^k = \sigma_{qzb}^{(k+1)} \quad q=\alpha,\beta,z \quad k=1,2,\ldots,N_l-1 \tag{15}$$

This group of models is denoted by 'LMN'. 'M' means mixed models based on RMVT.

2.5. Unified formulation

The considered theories can be all unified considering that CLT and FSDT are a peculiar case of ESL higher-order models. These latter models can be regarded as a particular case of LW models in which the number of layers is equal to one and the through-the-thickness polynomial approximation is performed via the classical base $\{z^r : r = 0,1,\ldots,N\}$. In the case of EDZN models, Murakami's function is also considered. Eqs. (1)–(3), (8) and (9) can be unified into the following compact notation:

$$\begin{aligned} &u_q^k = F_\tau u_{q\tau}^k \quad q=\alpha,\beta,z \quad \tau = t,b,r, \\ &\sigma_{qz}^k = F_\tau \sigma_{qz\tau}^k \quad r=2,3,\ldots,N \quad k=1,2,\ldots,N_l \end{aligned} \tag{16}$$

The governing equations are derived according to the chosen variational statement (either PVD or RMVT) in a general way that does not depend upon the approximation approach (ESL or LW) and the polynomial expansion order.

3. Governing equations

For the sake of brevity, the governing equations and the related mechanical and geometrical boundary conditions are derived via the PVD only. The extension to RMVT is straightforward and it can be found in Carrera [26,30]. Assuming the proposed unified approach and considering a generic pressure loading $\mathbf{p}^{kT} = \{p_{\alpha z}^k,\ p_{\beta z}^k, p_{zz}^k\}$ acting on the top $\left(\Sigma_k^t = \{(\alpha,\beta,\zeta_k) : \zeta_k = 1\}\right)$ and the bottom $\left(\Sigma_k^b = \{(\alpha,\beta,\zeta_k) : \zeta_k = -1\}\right)$ of each lamina, PVD reads:

$$\sum_{k=1}^{N_l} \int_{\Omega_k} \int_{h_k} \left(\delta \boldsymbol{\epsilon}_p^{kT} \boldsymbol{\sigma}_p^k + \delta \boldsymbol{\epsilon}_n^{kT} \boldsymbol{\sigma}_n^k\right) dz_k\, d\Omega_k = \sum_{k=1}^{N_l} \int_{\Sigma_k^b \bigcup \Sigma_k^t} \delta \mathbf{u}^{kT} \mathbf{p}^k\, d\Omega_k \tag{17}$$

being:

$$\boldsymbol{\epsilon}_p = \begin{Bmatrix} \epsilon_{\alpha\alpha} \\ \epsilon_{\beta\beta} \\ \gamma_{\alpha\beta} \end{Bmatrix} \quad \boldsymbol{\epsilon}_n = \begin{Bmatrix} \gamma_{\alpha z} \\ \gamma_{\beta z} \\ \epsilon_{zz} \end{Bmatrix} \quad \boldsymbol{\sigma}_p = \begin{Bmatrix} \sigma_{\alpha\alpha} \\ \sigma_{\beta\beta} \\ \sigma_{\alpha\beta} \end{Bmatrix} \quad \boldsymbol{\sigma}_n = \begin{Bmatrix} \sigma_{\alpha z} \\ \sigma_{\beta z} \\ \sigma_{zz} \end{Bmatrix} \tag{18}$$

'T' as superscript stands for the transposition operator. In the case of linear elastic material, stresses and strains are related via Hooke's generalised law:

$$\begin{aligned} \boldsymbol{\sigma}_p^k &= \widetilde{\mathbf{C}}_{pp}^k \boldsymbol{\epsilon}_p^k + \widetilde{\mathbf{C}}_{pn}^k \boldsymbol{\epsilon}_n^k \\ \boldsymbol{\sigma}_n^k &= \widetilde{\mathbf{C}}_{np}^k \boldsymbol{\epsilon}_p^k + \widetilde{\mathbf{C}}_{nn}^k \boldsymbol{\epsilon}_n^k \end{aligned} \tag{19}$$

Terms $\widetilde{\mathbf{C}}_{pp}^k$, $\widetilde{\mathbf{C}}_{pn}^k$, $\widetilde{\mathbf{C}}_{np}^k$ and $\widetilde{\mathbf{C}}_{nn}^k$ are the material stiffness matrices for a k-layer in the global reference system, see Carrera [26]. The displacement–strain relations are:

$$\begin{aligned} \boldsymbol{\epsilon}_p^k &= \mathbf{D}_p \mathbf{u}^k + \mathbf{A}_p \mathbf{u}^k \\ \boldsymbol{\epsilon}_n^k &= \mathbf{D}_{n\Omega} \mathbf{u}^k + \mathbf{A}_n \mathbf{u}^k + \mathbf{D}_{nz} \mathbf{u}^k \end{aligned} \tag{20}$$

in which $\mathbf{D}_p$, $\mathbf{D}_{n\Omega}$, and $\mathbf{D}_{nz}$ are differential matrix operators and $\mathbf{A}_p$ and $\mathbf{A}_n$ are geometrical terms accounting for the through-the-thickness variation of the curvature:

$$\begin{aligned} \mathbf{D}_p &= \begin{bmatrix} \frac{1}{H_\alpha^k}\frac{\partial}{\partial\alpha} & 0 & 0 \\ 0 & \frac{1}{H_\beta^k}\frac{\partial}{\partial\beta} & 0 \\ \frac{1}{H_\beta^k}\frac{\partial}{\partial\beta} & \frac{1}{H_\alpha^k}\frac{\partial}{\partial\alpha} & 0 \end{bmatrix}, \quad \mathbf{A}_p = \begin{bmatrix} 0 & 0 & \frac{1}{H_\alpha^k R_\alpha^k} \\ 0 & 0 & \frac{1}{H_\beta^k R_\beta^k} \\ 0 & 0 & 0 \end{bmatrix} \\ \mathbf{D}_{n\Omega} &= \begin{bmatrix} 0 & 0 & \frac{1}{H_\alpha^k}\frac{\partial}{\partial\alpha} \\ 0 & 0 & \frac{1}{H_\beta^k}\frac{\partial}{\partial\beta} \\ 0 & 0 & 0 \end{bmatrix}, \quad \mathbf{A}_n = \begin{bmatrix} -\frac{1}{H_\alpha^k R_\alpha^k} & 0 & 0 \\ 0 & -\frac{1}{H_\beta^k R_\beta^k} & 0 \\ 0 & 0 & 0 \end{bmatrix} \\ \mathbf{D}_{nz} &= \begin{bmatrix} \frac{\partial}{\partial z} & 0 & 0 \\ 0 & \frac{\partial}{\partial z} & 0 \\ 0 & 0 & \frac{\partial}{\partial z} \end{bmatrix} \end{aligned} \tag{21}$$

H_α^k and H_β^k account for the change in length of a k-layer segment due to the curvature:

$$H_\alpha^k = A^k\left(1 + \frac{z - z_{0k}}{R_\alpha^k}\right), \quad H_\beta^k = B^k\left(1 + \frac{z - z_{0k}}{R_\beta^k}\right) \tag{22}$$

where A^k and B^k are the coefficients of the first fundamental form of mid surface Ω_k of a k-layer. In the case of doubly curved shell with constant curvature radii, $A^k = B^k = 1$. No assumptions on curvature terms are made, they are fully retained in the present formulation. By replacing Eqs. (19) and (20) and the unified displacement field in Eq. (16) into Eq. (17) and after application of Gauss–Green's theorem [42], PVD reads:

$$\begin{aligned} &\sum_{k=1}^{N_l} \in_{\Omega_k} \delta\mathbf{u}_\tau^{kT} \int_{h_k} \Big\{ (-F_\tau \mathbf{D}_p^T + F_\tau \mathbf{A}_p^T)\Big[\widetilde{\mathbf{C}}_{pp}^k (F_s\mathbf{D}_p + F_s\mathbf{A}_p) \\ &+ \widetilde{\mathbf{C}}_{pn}^k (F_s\mathbf{D}_{n\Omega} + F_s\mathbf{A}_n + F_{s,z})\Big] + (-F_\tau \mathbf{D}_{n\Omega}^T + F_\tau \mathbf{A}_n^T + F_{\tau,z}) \\ &\times \Big[\widetilde{\mathbf{C}}_{np}^k (F_s\mathbf{D}_p + F_s\mathbf{A}_p) + \widetilde{\mathbf{C}}_{nn}^k (F_s\mathbf{D}_{n\Omega} + F_s\mathbf{A}_n + F_{s,z})\Big]\Big\} H_\alpha^k H_\beta^k dz_k \mathbf{u}_s^k d\Omega_k \\ &+ \sum_{k=1}^{N_l} \in_{\Gamma_k} \delta\mathbf{u}_\tau^{kT} \in_{h_k} \Big\{ F_\tau \mathbf{I}_p^T \Big[\widetilde{\mathbf{C}}_{pp}^k (F_s\mathbf{D}_p + F_s\mathbf{A}_p) + \widetilde{\mathbf{C}}_{pn}^k (F_s\mathbf{D}_{n\Omega} + F_s\mathbf{A}_n + F_{s,z})\Big] \\ &+ F_\tau \mathbf{I}_{n\Omega}^T \Big[\widetilde{\mathbf{C}}_{np}^k (F_s\mathbf{D}_p + F_s\mathbf{A}_p) + \widetilde{\mathbf{C}}_{nn}^k (F_s\mathbf{D}_{n\Omega} + F_s\mathbf{A}_n + F_{s,z})\Big]\Big\} H_\alpha^k H_\beta^k dz_k \mathbf{u}_s^k d\Omega_k \\ &= \sum_{k=1}^{N_l} \int_{\Sigma_k^b \bigcup \Sigma_k^t} \delta\mathbf{u}_\tau^{kT} \mathbf{p}_\tau^k d\Omega_k \end{aligned} \tag{23}$$

being:

$$\mathbf{I}_p = \begin{bmatrix} \frac{1}{H_\alpha^k} & 0 & 0 \\ 0 & \frac{1}{H_\beta^k} & 0 \\ \frac{1}{H_\beta^k} & \frac{1}{H_\alpha^k} & 0 \end{bmatrix} \quad \mathbf{I}_{n\Omega} = \begin{bmatrix} 0 & 0 & \frac{1}{H_\alpha^k} \\ 0 & 0 & \frac{1}{H_\beta^k} \\ 0 & 0 & 0 \end{bmatrix} \tag{24}$$

$\mathbf{p}_\tau^k$ is a load vector variationally consistent with applied loading $\mathbf{p}^k$. Eq. (23) yields the governing equations and the boundary conditions:

$$\begin{aligned} &\mathbf{K}_d^{k\tau s} \mathbf{u}_s^k = \mathbf{p}_\tau^k \\ &\mathbf{u}_\tau^k = \bar{\mathbf{u}}_\tau^k \quad (\alpha,\ \beta,\ z) \in \Gamma_k^g \\ &\mathbf{\Pi}_d^{k\tau s} \mathbf{u}_s^k = \mathbf{\Pi}_d^{k\tau s} \bar{\mathbf{u}}_s^k \quad (\alpha,\ \beta,\ z) \in \Gamma_k^m \end{aligned} \tag{25}$$

Geometrical boundary conditions, $\bar{\mathbf{u}}_\tau^k$, are applied on Γ_k^g and the mechanical ones, $\Pi_d^{k\tau s}\bar{\mathbf{u}}_s^k$, on Γ_k^m. Differential stiffness matrix and mechanical boundary conditions matrix are:

$$\begin{aligned} \mathbf{K}_d^{k\tau s} = \int_{h_k} \Big\{ &\Big(-F_\tau \mathbf{D}_p^T + F_\tau \mathbf{A}_p^T\Big)\Big[\widetilde{\mathbf{C}}_{pp}^k (F_s\mathbf{D}_p + F_s\mathbf{A}_p) \\ &+ \widetilde{\mathbf{C}}_{pn}^k (F_s\mathbf{D}_{n\Omega} + F_s\mathbf{A}_n + F_{s,z})\Big] + \Big(-F_\tau \mathbf{D}_{n\Omega}^T + F_\tau \mathbf{A}_n^T + F_{\tau,z}\Big) \\ &\times \Big[\widetilde{\mathbf{C}}_{np}^k (F_s\mathbf{D}_p + F_s\mathbf{A}_p) + \widetilde{\mathbf{C}}_{nn}^k (F_s\mathbf{D}_{n\Omega} + F_s\mathbf{A}_n + F_{s,z})\Big]\Big\} H_\alpha^k H_\beta^k dz_k \end{aligned} \tag{26}$$

$$\begin{aligned} \mathbf{\Pi}_d^{k\tau s} = \int_{h_k} \Big\{ &F_\tau \mathbf{I}_p^T \Big[\widetilde{\mathbf{C}}_{pp}^k (F_s\mathbf{D}_p + F_s\mathbf{A}_p) + \widetilde{\mathbf{C}}_{pn}^k (F_s\mathbf{D}_{n\Omega} + F_s\mathbf{A}_n + F_{s,z})\Big] \\ &+ F_\tau \mathbf{I}_{n\Omega}^T \Big[\widetilde{\mathbf{C}}_{np}^k (F_s\mathbf{D}_p + F_s\mathbf{A}_p) + \widetilde{\mathbf{C}}_{nn}^k (F_s\mathbf{D}_{n\Omega} + F_s\mathbf{A}_n + F_{s,z})\Big]\Big\} H_\alpha^k H_\beta^k dz_k \end{aligned} \tag{27}$$

Eq. (25) are solved via a Navier-type solution upon assumption of the following harmonic form for the applied loadings and unknown displacements:

$$\begin{aligned} \left(u_\alpha^k, p_{\alpha z}^k\right) &= \sum_{m=1}^{\bar{m}} \sum_{n=1}^{\bar{n}} \left(U_\alpha^k(z), P_{\alpha z}^k(z)\right) \cos\left(\frac{m\pi}{a}\alpha\right) \sin\left(\frac{n\pi}{b}\beta\right) \\ \left(u_\beta^k, p_{\beta z}^k\right) &= \sum_{m=1}^{\bar{m}} \sum_{n=1}^{\bar{n}} \left(U_\beta^k(z), P_{\beta z}^k(z)\right) \sin\left(\frac{m\pi}{a}\alpha\right) \cos\left(\frac{n\pi}{b}\beta\right) \end{aligned} \tag{28}$$

Thanks to the problem linearity, Navier's solution can be assumed for any general loading whose Fourier's series expansion is known, (see Carrera et al. [27,28]). The convergence of the Navier's solution depends on several factors such as type of the loading, shell thickness and stacking sequence.

4. Results and discussion

The static analysis of simply supported, laminated doubly curved shells is addressed. Geometrical data are: $a/b = 1$ and $R_\alpha = R_\beta = R$. All the plies have the same thickness. Three laminations are investigated: [0/90], [0/90/0] and $[0/90]_s$. Stacking sequence starts from shell top. Fibres' orientation is measured toward α-axis. Layers are all made of the same material whose mechanical properties are: $E_L = 25E_T$, $G_{LT} = 0.5E_T$, $G_{TT} = 0.2E_T$, $\nu_{LT} = 0.25$ and $\nu_{TT} = 0.49$. Subscript 'L' stands for direction parallel to the fibres, while 'T' identifies the direction transverse to them. Shells are subjected to bi-sinusoidal and distributed or localised uniform bending loadings. A point load is also considered. Loadings are all applied at shell top. Side-to-thickness (a/h) and curvature-radius-to-side (R/a) ratios are assumed as analysis parameters. Thin ($a/h = 100$) and relatively thick ($a/h = 10$) shells are investigated. R/a is as low as 5 (deep shells). The limit case in which a shell degenerates into a plate ($R/a \to \infty$) is also accounted for. In this case, results are assessed towards Pagano's 3D exact solution (see Pagano [43]). Results are also compared with the higher-order model 'HSDT' by

Reddy and Liu [15]. Unless differently stated, $\bar{u}_z$ and $\bar{\sigma}_{zz}$ are evaluated at $(a/2, b/2, 0)$ and $\bar{\sigma}_{\alpha\alpha}$ is evaluated at $(a/2, b/2, h/2)$. Transverse shear stresses $\bar{\sigma}_{\alpha z}$ and $\bar{\sigma}_{\beta z}$ are evaluated at $(0, b/2, 0)$ and $(a/2, 0, 0)$, respectively. Shear stress component $\bar{\sigma}_{\alpha\beta}$ is computed at $(0, 0, h/2)$. The transverse stress components in PVD-based models are evaluated by means of the constitutive equations, whereas, in the case of RMVT-based models, they are primary variables.

4.1. Bi-sinusoidal loading

A bi-sinusoidal loading with $\bar{m} = \bar{n} = 1$ in Eq. (28) is considered. Displacements and stresses are put in a non-dimensional form as follows:

$$\bar{u}_z = 10^3 \frac{E_T h^3}{P_{zz} a^4} u_z \tag{29}$$

$$(\bar{\sigma}_{\alpha\alpha}, \bar{\sigma}_{\alpha\beta}, \bar{\sigma}_{\alpha z}, \bar{\sigma}_{\beta z}) = \frac{h^2}{P_{zz} a^2} (\sigma_{\alpha\alpha}, \sigma_{\alpha\beta}, \sigma_{\alpha z}, \sigma_{\beta z}), \quad \bar{\sigma}_{zz} = \frac{\sigma_{zz}}{P_{zz}} \tag{30}$$

Tables 1 and 2 present the dimensionless central deflection in a [0/90/0] thin and relatively thick shell. As far as LW models are concerned, results converge for N as low as three. They match Pagano's solution within the considered number of significant digits. For sake of brevity, LM2 and LD2 models are not reported. In the case of relatively thick shells, they differ from the converged solution by about 0.1%, at worst. The same consideration holds for ED3, ED3D and EDZ2 theories when compared with the corresponding higher-order approximation. Murakami's function improves the accuracy for an expansion order higher than the first one. On the contrary, EDZ1 degrades the accuracy of the solution for $a/h = 100$. A first-order approximation (with or without Murakami's function) is here reported for the sake of completeness. It accounts for a constant (or a piece-wise constant) through-the-thickness transverse deformation and, therefore, should be regarded as a transition between CTs and higher-order models. CTs yield a good approximation for thin shells, whereas, in the case of $a/h = 10$, they differ from the converged solution by about 15%, at best. Results for a $[0/90]_s$ stacking sequence are similar to those addressed in Tables 1 and 2. Fig. 2 presents the dimensionless central deflection along the thickness for this latter stacking sequence, $a/h = 10$ and $R/a = 5$. Dimensionless central deflection versus $(R/a)^{-1}$ for a [0/90] lamination and $a/h = 10$ is reported in Fig. 3. For this stacking sequence, FSDT yields good results. It differ from fourth-order LW model by about 1.4%. Decreasing R/a, HSDT by Reddy and Liu [15] degrades since governing equations are obtained through a modified version of Sanders' theory [44]. Table 3 presents the dimensionless stresses in a [0/90/0] shell for $a/h = 100$. As far as LW models are concerned, results converge for N as low as three. In the case of plate, they match Pagano's solution. Results for $\bar{\sigma}_{\alpha\alpha}$ are in good agreement for all the theories since a thin shell is considered. In the case of transverse shear stress component $\bar{\sigma}_{\alpha z}$, LW theories yield results in good agreement, the difference between first- and third-order being about 0.5%. The lower R/a, the higher the difference between LMN and LDN models. For instance, LD3 theory differ from LM3 by about 4.6%. Since curvature terms are exactly retained in the geometry description of both models, this discrepancy is directly related to the lack of inter-layer equilibrium in LDN. $\bar{\sigma}_{\alpha z}$ computed via EDN, EDND and FSDT is inaccurate. Fig. 4 shows $\bar{\sigma}_{\alpha z}$ versus z/h. $\bar{\sigma}_{\beta z}$ is smaller than $\bar{\sigma}_{\alpha z}$ since it acts on a plane that is less stiff than the $\alpha - z$ one. Results are more widespread than for the case of $\bar{\sigma}_{\alpha z}$. For instance, in the case of a deep shell $\bar{\sigma}_{\beta z}$ via LD4 model is about 55% lower than that computed by LM4 theory. Higher-order, LW mixed models are required for doubly curved shells. LDN models are accurate in the case of plates. Stress field in a [0/90/0] shell with $a/h = 10$ is presented in Tables 4 and 5. LW models yield accurate results for an approximation order as low as two. As far as stresses on the reference surface are concerned, third- or

Table 1
Dimensionless deflection $\bar{u}_z$ for [0/90/0] shell under bi-sinusoidal loading, $a/h = 100$.

R/a	5	10	20	50	∞
Pagano	–	–	–	–	4.3471
HSDT [15]	1.0321	2.4099	3.1670	4.2071	4.3420
LM3/4, LD3/4	1.0364	2.4166	3.6239	4.2130	4.3471
LM1	1.0363	2.4158	3.6223	4.2109	4.3449
LD1	1.0353	2.4108	3.6110	4.1957	4.3287
EDZ3	1.0363	2.4165	3.6238	4.2130	4.3471
EDZ1	1.0278	2.3702	3.5206	4.0740	4.1992
ED4	1.0361	2.4150	3.6206	4.2086	4.3424
ED1	1.0383	2.4158	3.6160	4.2001	4.3329
ED4D	1.0361	2.4151	3.6208	4.2089	4.3427
ED2D	1.0355	2.4120	3.6140	4.1997	4.3329
CTs	1.0355	2.4120	3.6139	4.1997	4.3329

Table 2
Dimensionless deflection $\bar{u}_z$ for [0/90/0] shell under bi-sinusoidal loading, $a/h = 10$.

R/a	5	10	20	50	∞
Pagano	–	–	–	–	7.5164
HSDT [15]	6.7688	7.0325	7.1016	7.1212	7.1250
LM3/4, LD3/4	7.3120	7.4978	7.5290	7.5267	7.5164
LM1	7.2790	7.4631	7.4940	7.4917	7.4814
LD1	7.1526	7.3284	7.3573	7.3547	7.3445
EDZ3	7.3477	7.5153	7.5365	7.5281	7.5135
EDZ1	6.9599	7.1359	7.1678	7.1678	7.1598
ED4	6.9573	7.1230	7.1499	7.1472	7.1374
ED1	6.1844	6.3030	6.3195	6.3149	6.3059
ED4D	7.0014	7.1661	7.1911	7.1867	7.1757
ED2D	6.1904	6.3074	6.3220	6.3160	6.3059
CTs	6.1895	6.3072	6.3219	6.3160	6.3059

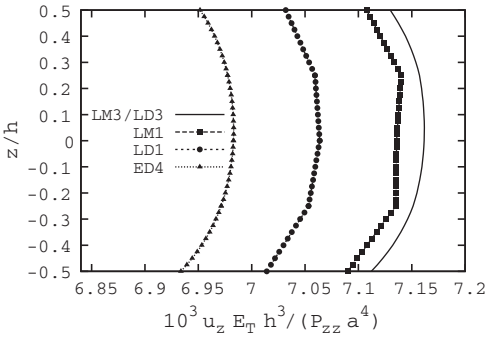

Fig. 2. Dimensionless deflection $\bar{u}_z$ along the thickness at $(a/2, b/2)$ for $[0/90]_s$ shell, $a/h = 10$, $R/a = 5$, bi-sinusoidal loading.

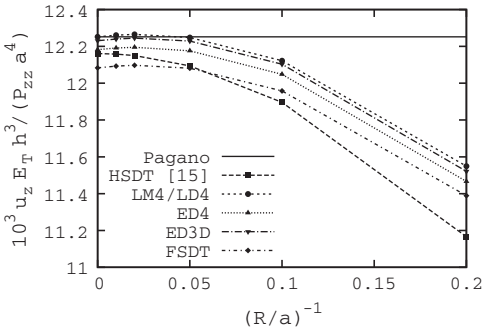

Fig. 3. Dimensionless deflection $\bar{u}_z$ versus $(R/a)^{-1}$ for [0/90] shell, $a/h = 10$, bi-sinusoidal loading.

Table 3
Dimensionless stresses for $a/h = 100$, [0/90/0] shell under bi-sinusoidal loading.

	$\bar{\sigma}_{\alpha\alpha}$			$\bar{\sigma}_{\alpha z}$			$\bar{\sigma}_{\beta z}$		
	$\times 10$	$\times 10$	$\times 10$	$\times 10^4$	$\times 10^3$	$\times 10^3$	$\times 10^5$	$\times 10^4$	$\times 10^4$
R/a	5	20	∞	5	20	∞	5	20	∞
Pagano	–	–	5.3923	–	–	3.9468	–	–	8.2828
LM3/4	1.5570	4.7360	5.3923	9.3729	3.2893	3.9468	19.678	6.9032	8.2828
LM1	1.5592	4.7426	5.3999	9.3332	3.2745	3.9287	15.734	5.5164	6.6182
LD3/4	1.5570	4.7360	5.3923	8.9390	3.2514	3.9468	8.8321	5.9547	8.2828
LD1	1.5625	4.7445	5.3998	8.9172	3.2356	3.9248	5.0618	4.6166	6.6685
EDZ3	1.5581	4.7371	5.3926	9.0579	3.2938	3.9977	6.6562	5.1758	7.3450
EDZ1	1.5667	4.6759	5.2968	8.9989	3.2058	3.8687	3.5458	4.0809	6.0275
ED4	1.5586	4.7366	5.3914	6.2343	2.3011	2.8061	6.6333	5.1734	7.3428
ED1	1.5668	4.7381	5.3845	2.9437	1.1434	1.4159	3.1324	3.9376	5.8559
ED(3/4)D	1.5592	4.7372	5.3918	6.2351	2.3012	2.8062	6.6333	5.1734	7.3428
FSDT	1.5596	4.7325	5.3846	2.9368	1.1428	1.4159	3.1324	3.9376	5.8559

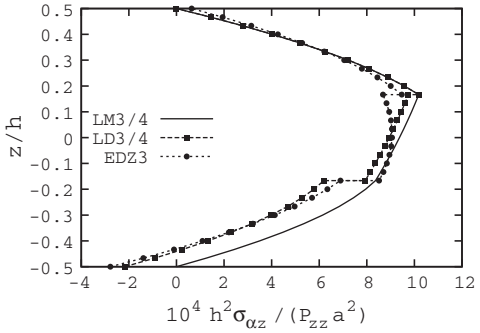

Fig. 4. Dimensionless transverse shear stress $\bar{\sigma}_{xz}$ along the thickness at $(0, b/2)$ for [0/90/0] shell, $a/h = 100$, $R/a = 5$, bi-sinusoidal loading.

fourth-order approximations are required for ESL theories. These models cannot be assumed for evaluating the transverse shear stress component. The accuracy of LW in predicting $\bar{\sigma}_{zz}$ depends upon R/a. For deep shells, a second-order, mixed model is required at least. In the case of $R/a \geqslant 20$, displacement based models yield accurate results. The variation of transverse shear and normal stress components versus the through-the-thickness coordinate for a [0/90] and a $[0/90]_s$ laminate are presented in Figs. 5 and 6, respectively. It should be noticed that LM4 model satisfies the mechanical boundary conditions.

4.2. Distributed and localised uniform loading

Spherical shells subjected to a distributed uniform loading are investigated first. A Fourier approximation with $\bar{m}$ and $\bar{n}$ in Eq. (28) equal to 29 is used. This value has been chosen in order to ensure the convergence of the transverse displacement via Pagano's solution with five significant digits for all the considered configurations. It has been found that convergence depends upon the stacking sequence and the side-to-thickness ratio. The higher the

Table 4
Dimensionless stresses $\bar{\sigma}_{xx}$ and $\bar{\sigma}_{x\beta}$ for $a/h = 10$, [0/90/0] shell under bi-sinusoidal loading.

	$10 \times \bar{\sigma}_{\alpha\alpha}$					$-100 \times \bar{\sigma}_{\alpha\beta}$				
R/a	5	10	20	50	∞	5	10	20	50	∞
Pagano	–	–	–	–	5.8836	–	–	–	–	2.8628
LM4, LD4	5.8032	5.9161	5.9187	5.9021	5.8836	1.4235	2.1570	2.5166	2.7264	2.8628
LM1	5.7736	5.8856	5.8882	5.8633	5.8533	1.4115	2.1417	2.4998	2.7770	2.8446
LD1	5.6325	5.7382	5.7398	5.7152	5.7055	1.3719	2.0873	2.4383	2.7102	2.7765
EDZ2	5.3990	5.4855	5.4785	5.4575	5.4366	1.3187	2.0192	2.3639	2.5654	2.6969
ED4	5.7757	5.8630	5.8554	5.8338	5.8122	1.4066	2.0992	2.4384	2.6363	2.7651
ED2	5.1496	5.2059	5.1938	5.1734	5.1542	1.2380	1.8431	2.1397	2.3133	2.4266
ED4D	5.8194	5.9037	5.8936	5.8701	5.8473	1.4375	2.1367	2.4785	2.6777	2.8072
ED2D	5.1828	5.2323	5.2164	5.1934	5.1725	1.2617	1.8714	2.1698	2.3442	2.4580
FSDT	5.1932	5.2379	5.2192	5.1841	5.1725	1.2522	1.8666	2.1674	2.4009	2.4580

Table 5
Dimensionless stresses $\bar{\sigma}_{xz}$ and $\bar{\sigma}_{zz}$ for $a/h = 10$, [0/90/0] shell under bi-sinusoidal loading.

	$100 \times \bar{\sigma}_{\alpha z}$					$10 \times \bar{\sigma}_{zz}$				
R/a	5	10	20	50	∞	5	10	20	50	∞
Pagano	–	–	–	–	3.5674	–	–	–	–	4.9908
LM4	3.4588	3.5564	3.5732	3.5724	3.5674	2.4516	3.6840	4.3342	4.7282	4.9908
LM1	3.4416	3.5384	3.5550	3.5522	3.5492	2.6403	3.7821	4.3844	4.8711	4.9926
LD4	3.4281	3.5404	3.5651	3.5690	3.5671	2.5557	3.7111	4.3412	4.7294	4.9908
LD1	3.4251	3.5342	3.5578	3.5609	3.5594	2.6830	3.7781	4.3751	4.8668	4.9908
ED4	2.5088	2.5904	2.6090	2.6127	2.6119	2.6666	3.7727	4.3763	4.7482	4.9987
ED1	1.3144	1.3565	1.3674	1.3709	1.3710	3.5203	4.2138	4.5952	4.9109	4.9909
ED4D	2.5198	2.6015	2.6200	2.6234	2.6225	1.3625	0.6723	0.3310	0.1308	0.0000
ED2D	1.3149	1.3569	1.3676	1.3705	1.3710	1.1987	0.5887	0.2895	0.1143	0.0000
FSDT	1.3146	1.3568	1.3676	1.3709	1.3710	1.1856	0.5821	0.2862	0.0562	0.0000

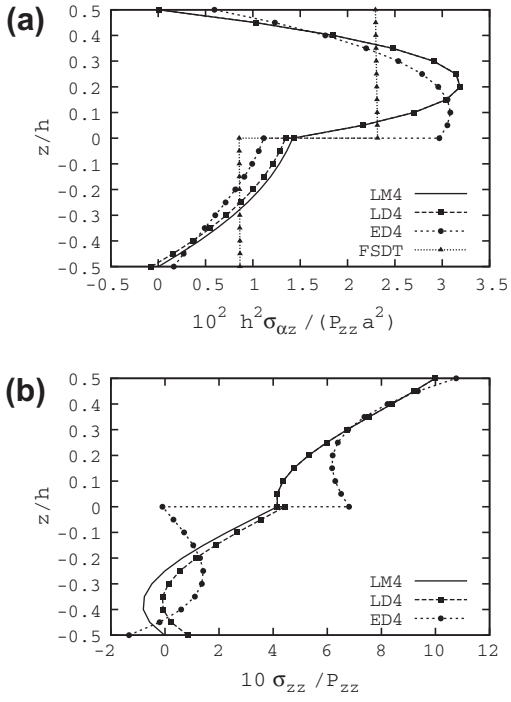

Fig. 5. Dimensionless transverse stress (a) $\bar{\sigma}_{xz}$ and (b) $\bar{\sigma}_{zz}$ along the thickness at $(0,b/2)$ and at $(a/2,b/2)$, respectively. [0/90] shell, $a/h = 10$, $R/a = 5$, bi-sinusoidal loading.

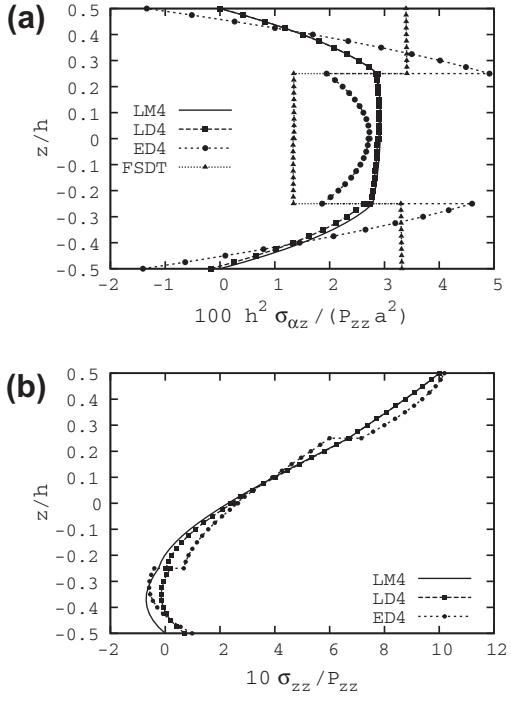

Fig. 6. Dimensionless transverse stress (a) $\bar{\sigma}_{xz}$ and (b) $\bar{\sigma}_{zz}$ along the thickness at $(0,b/2)$ and at $(a/2,b/2)$, respectively. $[0/90]_s$ shell, $a/h = 10$, $R/a = 5$, bi-sinusoidal loading.

number of plies, the higher the value of $\bar{m}$ and $\bar{n}$. Increasing a/h, a smaller value is required. Displacements and stresses are put in the same non-dimensional form as shown in Eqs. (29) and (30). Tables 6 and 7 present the dimensionless central deflection in a [0/90/0] shell. As far as LW models are concerned, results converge for N as low as three. They match Pagano's solution within the considered number of significant digits for both thin and relatively thick shells. EDZ3 model yields accurate results for $a/h = 10$ and any value of R/a. Results computed via the other ESL theories are inaccurate. For instance, the difference between FSDT and the converged solution is about 15% at best. It is about 5% in the case of ED4 model. Fig. 7 presents the dimensionless central deflection along the thickness for $a/h = 10$ and $R/a = 5$. The stacking sequence is [0/90]. The deflection computed on the reference surface via ED4D model is closer to the converged solution than the one obtained via ED4, as also in Table 7. This is not the case for different values of the through-the-thickness coordinate. Tables 8 and 9 present the dimensionless stresses in a [0/90/0] shell for $a/h = 100$ and 10, respectively. ESL theories are accurate for $\bar{\sigma}_{\alpha\alpha}$ but not for transverse shear stresses. The only exception is represented by $\bar{\sigma}_{\alpha z}$ computed via EDZN theories that differs from higher-order LW mixed models by less than 3%. An accurate prediction of $\bar{\sigma}_{zz}$ for deep shells calls for a LM4 model. For shallow shells, all the considered

Table 6
Dimensionless central deflection $\bar{u}_z$ for [0/90/0] shell under distributed uniform loading, $a/h = 100$.

R/a	5	10	20	50	∞
Pagano	–	–	–	–	6.7127
HSDT [15]	1.5118	3.6445	5.5473	6.6421	6.6970
LM3/4, LD3/4	1.5155	3.6528	5.5610	6.4988	6.7127
LM1	1.5153	3.6518	5.5585	6.6548	6.7092
LD1	1.5148	3.6465	5.5443	6.6336	6.6876
EDZ3	1.5154	3.6528	5.5610	6.4989	6.7128
EDZ1	1.5104	3.6027	5.4291	6.3131	6.5134
ED4	1.5152	3.6507	5.5560	6.4921	6.7055
ED2	1.5147	3.6465	5.5460	6.4783	6.6908
ED4D	1.5151	3.6507	5.5562	6.4924	6.7058
FSDT	1.5146	3.6464	5.5459	6.6368	6.6909

Table 7
Dimensionless central deflection $\bar{u}_z$ for [0/90/0] shell under distributed uniform loading, $a/h = 10$.

R/a	5	10	20	50	∞
Pagano	–	–	–	–	11.525
HSDT [15]	10.332	10.752	10.862	10.893	10.899
LM3/4, LD3/4	11.191	11.491	11.542	11.540	11.524
LM1	11.083	11.379	11.430	11.422	11.412
LD1	10.958	11.242	11.290	11.280	11.271
EDZ3	11.273	11.535	11.566	11.550	11.526
EDZ1	10.677	10.961	11.013	11.013	11.001
ED4	10.640	10.907	10.951	10.948	10.933
ED2	9.4239	9.6167	9.6448	9.6388	9.6253
ED4D	10.695	10.961	11.003	10.997	10.981
FSDT	9.4495	9.6402	9.6655	9.6506	9.6419

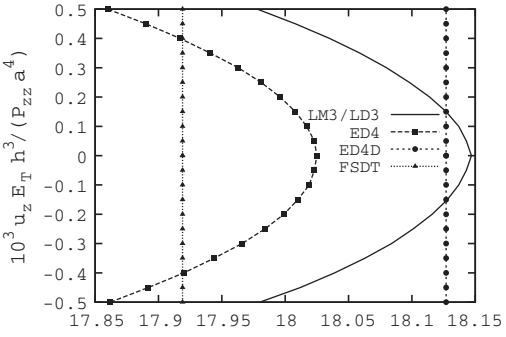

Fig. 7. Dimensionless deflection $\bar{u}_z$ along the thickness at $(a/2,b/2)$ for [0/90] shell, $a/h = 10$, $R/a = 5$, distributed uniform loading.

Table 8
Dimensionless stresses for $a/h = 100$, [0/90/0] shell under distributed uniform loading.

	$\bar{\sigma}_{\alpha\alpha}$			$\bar{\sigma}_{\alpha z}$			$\bar{\sigma}_{\beta z}$		
	$\times 10$	$\times 10$	$\times 10$	$\times 10^4$	$\times 10^3$	$\times 10^3$	$\times 10^4$	$\times 10^3$	$\times 10^3$
R/a	5	20	∞	5	20	∞	5	20	∞
Pagano	–	–	8.0831	–	–	7.2115	–	–	3.8787
LM4	1.9719	6.9720	8.0839	24.751	6.1677	7.2116	19.984	3.5590	3.8789
LM1	1.9738	6.9787	8.0919	24.666	6.1443	7.1833	14.916	2.7006	2.9515
LD4	1.9719	6.9720	8.0839	24.065	6.1080	7.2115	17.616	3.3777	3.8798
LD1	1.9786	6.9827	8.0920	24.046	6.0887	7.1833	12.735	2.5364	2.9679
EDZ3	1.9733	6.9735	8.0841	24.415	6.1930	7.3105	13.447	2.6748	3.1221
EDZ2	1.9941	6.9050	7.9552	24.186	6.0608	7.1172	13.027	2.5739	3.0000
ED4	1.9742	6.9734	8.0830	17.070	4.3429	5.1443	13.541	2.7167	3.1725
ED1	1.9869	6.9771	8.0735	8.3562	2.1692	2.6012	9.6223	2.0300	2.4255
ED4D	1.9747	6.9736	8.0830	17.072	4.3429	5.1443	13.544	2.7174	3.1733
ED2D	1.9766	6.9681	8.0736	8.3454	2.1682	2.6012	9.6098	2.0294	2.4255
FSDT	1.9767	6.9682	8.0736	8.3442	2.1682	2.6012	9.6110	2.0295	2.4255

Table 9
Dimensionless stresses for $a/h = 10$, [0/90/0] shell under distributed uniform loading.

	$10 \times \bar{\sigma}_{\alpha\alpha}$			$10^2 \times \bar{\sigma}_{\alpha z}$			$10^2 \times \bar{\sigma}_{zz}$		
R/a	5	20	∞	5	20	∞	5	20	∞
Pagano	–	–	8.6842	–	–	6.2815	–	–	5.0381
LM4	8.5121	8.7268	8.6820	6.1266	6.3042	6.2926	1.2835	4.0665	5.0411
LM1	8.4493	8.6654	8.6224	6.0640	6.2389	6.2272	1.5297	4.1352	5.0470
LD4	8.5120	8.7267	8.6818	6.0628	6.2788	6.2805	1.4403	4.0740	5.0380
LD1	8.3025	8.5037	8.4600	6.0514	6.2606	6.2616	1.5914	4.1112	5.0328
ED4	8.4697	8.6283	8.5709	4.5157	4.6738	4.6772	1.5022	4.1000	5.0484
ED1	7.7557	7.8284	7.7658	2.4598	2.5415	2.5462	2.7991	4.4742	5.0909
ED4D	8.5298	8.6829	8.6219	4.5566	4.7127	4.7149	1.9653	0.4774	0.0000
ED2D	7.7474	7.8340	7.7757	2.4611	2.5419	2.5462	1.7287	0.4172	0.0000
FSDT	7.7606	7.8376	7.7757	2.4606	2.5419	2.5462	1.7120	0.4129	0.0000

LW models yield results that differ by less than 1.5%. In this latter case, third- and fourth-order ED models are also accurate. Variation of stress components versus the through-the-thickness coordinate is not reported since it is similar to that addressed in Figs. 5 and 6. Figs. 8 and 9 present the transverse dimensionless displacement versus $2\alpha/a$ and $2\beta/b$ at shell top for [0/90/0] and $[0/90]_s$ stacking sequences. Shells are subjected to a localised uniform loading. Loading application area is such that $3/8 \leqslant \alpha/a, \beta/b \leqslant 5/8$. $\bar{m}$ and $\bar{n}$ in Eq. (28) are equal to 101. This value ensures a convergence of the maximum value of the displacement with an accuracy of five significant digits. The curvature of transverse displacement changes in correspondence of the boundary of the loading application area. For a [0/90/0] laminate, the change in curvature is more evident varying β than α. This difference is less evident in the case of a $[0/90]_s$ stacking sequence. Higher-order theories converge to the same results moving away from the loading application area.

4.3. Point load

A point load is considered. $\bar{m}$ and $\bar{n}$ in Eq. (28) are equal to 101 as in Reddy and Liu [15]. Displacements and stresses are put in a non-dimensional form as follows:

$$\bar{u}_z = 10^2 \frac{E_T h^3}{P_{zz} a^2} u_z \tag{31}$$

$$(\bar{\sigma}_{\alpha\alpha}, \bar{\sigma}_{\alpha z}) = \frac{h^4}{P_{zz} a^2} (\sigma_{\alpha\alpha}, \sigma_{\alpha z}) \tag{32}$$

For the sake of brevity, only a moderately thick shell ($a/h = 10$) is investigated. A [0/90/0] stacking sequence is considered. The presented results change little versus R/a. Results for deep shells and plates can be barely distinguished. Only the case $R/a = 5$ is, therefore, presented. Point load induces high gradients in the displacement and stress field in the neighbourhood of shell top. For some of these quantities, LM4 results do not converge to

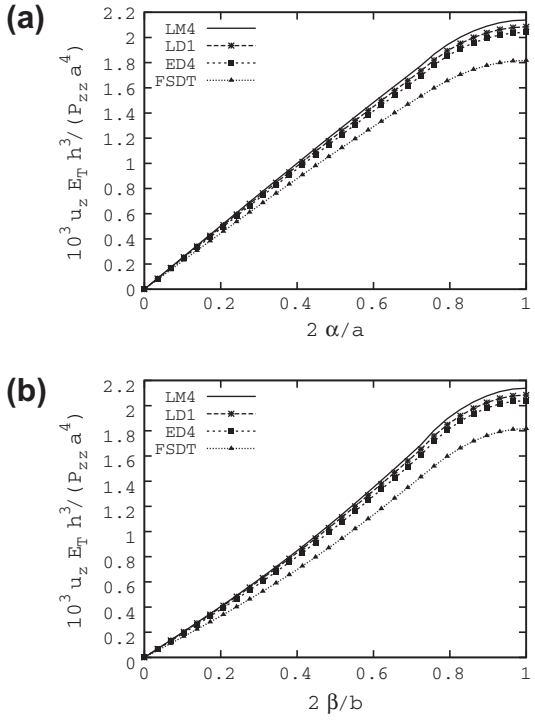

Fig. 8. Dimensionless transverse displacement $\bar{u}_z$ versus (a) $2\alpha/a$ at $\beta = b/2$, $z = 0$ and versus (b) $2\beta/b$ at $\alpha = a/2$, $z = 0$ for a [0/90/0] shell, $a/h = 10$, $R/a = 5$, localised uniform loading.

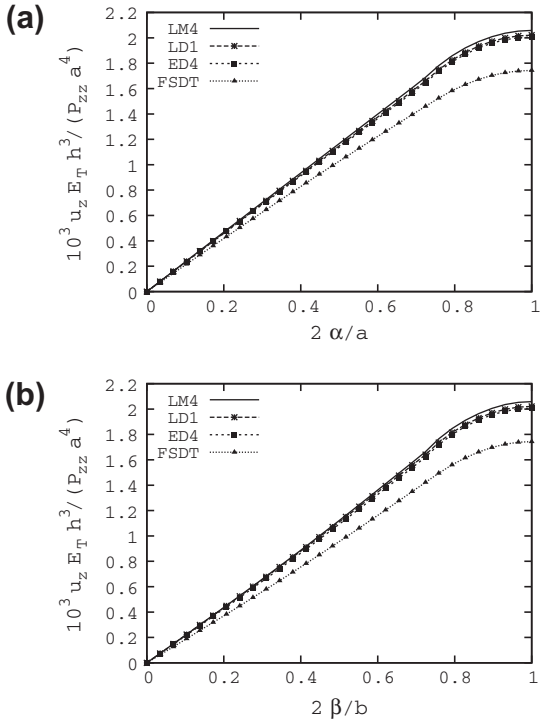

Fig. 9. Dimensionless transverse displacement $\bar{u}_z$ versus (a) $2\alpha/a$ at $\beta = b/2$, $z = 0$ and versus (b) $2\beta/b$ at $\alpha = a/2$, $z = 0$ for a $[0/90]_s$ shell, $a/h = 10$, $R/a = 5$, localised uniform loading.

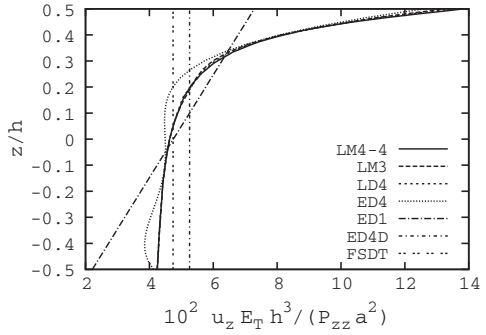

Fig. 10. Dimensionless transverse displacement $\bar{u}_z$ along the thickness at $(a/2, b/2)$ for [0/90/0] shell, $a/h = 10$, $R/a = 5$, point loading.

Pagano's solution. The top layer is fictitiously divided into computational layers to obtain a converging solution. Hereafter LM4-$\overline{N}$ stands for a LM4 model with the top physical layer divided into $\overline{N}$ computational layers. The LM4-$\overline{N}$ model that converges to Pagano's solution ($R/a \to \infty$) is chosen as reference solution. Fig. 10 presents the transverse dimensionless displacement. Four computational layers are required. LM3 and LD4 model converge to the reference solution (LM4-4) except for near the shell top. Higher-order ED theories, though not converging to the reference solution, are able to describe the increases of transverse displacement near the shell top. Fig. 11 presents the stress $\bar{\sigma}_{\alpha\alpha}$. In order to have a converged solution, ten computational layers are required, at least. LW models with less computational layers yield results oscillating around the reference solution. ESL theories cannot model the high gradient. Fig. 12 presents the transverse stress $\bar{\sigma}_{\alpha z}$. Because of the mechanical boundary conditions, $\bar{\sigma}_{\alpha z}$ should be zero at shell top and bottom. These conditions are not a-priori imposed in the proposed analytical solution. They are satisfied indirectly as long as

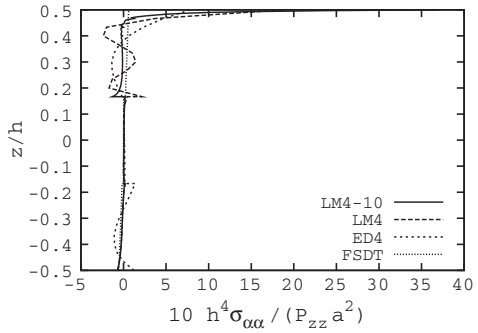

Fig. 11. Dimensionless inplane stress $\bar{\sigma}_{\alpha\alpha}$ along the thickness at $(a/2, b/2)$ for [0/90/0] shell, $a/h = 10$, $R/a = 5$, point loading.

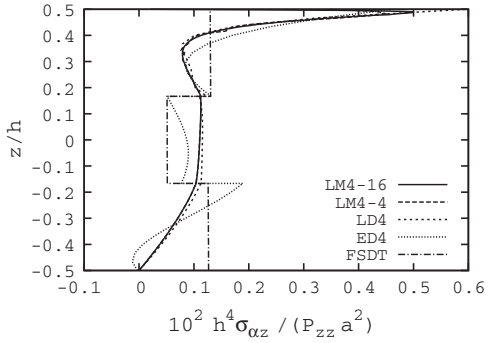

Fig. 12. Dimensionless transverse stress $\bar{\sigma}_{\alpha z}$ along the thickness at $(0, b/2)$ for [0/90/0] shell, $a/h = 10$, $R/a = 5$, point loading.

the expansion order yields an accurate solution in a global sense. This condition is satisfied only via *16* computational layers at least. Higher-order ESL theories fulfil the boundary condition at shell bottom.

5. Conclusions

A unified approach to formulate 2D shell theories has been here addressed. This formulation accounts for: (1) the type of main unknowns (displacements or displacements and transverse normal and shear stresses), (2) the approximation level (Equivalent Single Layer, ESL, or Layer-Wise, LW, approach), and (3) the a-priori through-the-thickness approximation order. According to these aspects, it is possible to formulate higher-order theories that: a- model the transverse shear as well as the normal deformation, b- ensure the continuity of the transverse normal and shear stresses, c- model the peculiar through-the-thickness zig-zag behaviour of displacements and transverse normal and shear stress components. Classical theories based upon Love's or Mindlin's kinematic hypotheses are derived as particular cases. Simply supported, doubly curved shells made of orthotropic materials have been investigated. Distributed and localised loadings and several stacking sequences have been considered. Analyses are carried out considering several values of the side-to-thickness and the curvature-radius-to-side ratios. Results have been compared with reference solutions present in literature. A hierarchy among the proposed 2D models have been established on the basis on their accuracy. LW models are mandatory for an accurate description of the stress field. When high stress gradients along the thickness are present, the accuracy of LW models, for a fixed approximation order, can be enhanced via fictitious computational layers. Murakami's zig-zag function increases the results accuracy for an approximation

order higher than the first one. Higher-order models are required for predicting the change in curvature of the transverse displacement due to localised loadings. Classical models yield good results for thin shallow shells. The presented results could be useful as benchmark for the validation of new theories and shell finite elements.

Acknowledgments

First and second authors are supported by the National Research Funding of Luxembourg (FNR) via the project CORE 2009 C09/MS/05 FUNCTIONALLY and under the AFR Grant PHD-08-069 BFR08/071, respectively.

References

[1] Timoshenko SP, Woinowsky-Krieger S. Theory of plates and shells. McGraw-Hill International Editions; 1959.
[2] Love AEH. The small free vibrations and deformation of a thin elastic shell. Philos Trans Roy Soc London A 1888;179:491–546.
[3] Love AEH. A treatise on the mathematical theory of elasticity. Cambridge University Press; 1906.
[4] Mindlin E. Influence of the rotatory inertia and shear in flexural motions of isotropic elastic plates. J Appl Mech 1951;18:1031–6.
[5] Bhimaraddi A. Three-dimensional elasticity solution for static response of orthotropic doubly curved shallow shells on rectangular planform. Compos Struct 1993;24(1):67–77.
[6] Wu CP, Tarn JQ, Chi SM. Three-dimensional analysis of doubly curved laminated shells. J Eng Mech 1996;122(5):391–401.
[7] Wu CP, Tarn JQ, Chi SM. An asymptotic theory for dynamic response of doubly curved laminated shells. Int J Solids Struct 1996;33(26):3813–41.
[8] Wu CP, Tarn JQ, Tang SC. A refined asymptotic theory for dynamic response of doubly curved laminated shells. Int J Solids Struct 1998;35(16):1953–79.
[9] Wu CP, Chi YW. Asymptotic solutions of laminated composite shallow shells with various boundary conditions. Acta Mech 1999;132:1–18.
[10] Grigolyuk EI, Kulikov GM. General direction of the development of the theory of shells. Mekh Kompozitnykh Mater 1988;2:287–98.
[11] Kapania RK. A review on the analysis of laminated shells. J Press Vess Technol 1989;111:88–96.
[12] Noor AK, Burton WS. Assessment of computational models for multilayered composite shells. Appl Mech Rev 1990;43:67–97.
[13] Noor AK, Burton WS, Bert CW. Computational models for sandwich panels and shells. Appl Mech Rev 1996;49:155–99.
[14] Carrera E. Theories and finite elements for multilayered plates and shells. Arch Comput Methods Eng 2002;9(2):87–140.
[15] Reddy JN, Liu CF. A higher-order shear deformation theory of laminated elastic shells. Int J Eng Sci 1985;23:319–30.
[16] Khdeir AA, Librescu L, Frederick D. A shear deformable theory of laminated composite shallow shell-type panels and their response analysis ii: Static response. Acta Mech 1989;77:1–12.
[17] Chaudhuri RZ, Abu-Arja KR. Exact solution of shear-flexible doubly curved anti-symmetric angle-ply shells. Int J Eng Sci 1988;26(6):587–604.
[18] Chaudhuri RZ, Kabir HRH. On analytical solutions to boundary-value problems of doubly-curved moderately-thick orthotropic shells. Int J Eng Sci 1989;27(11):1325–36.
[19] Chaudhuri RZ, Kabir HRH. Sensitivity of the response of moderately thick cross-ply doubly-curved panels to lamination and boundary constraint – i. Theory. Int J Solids Struct 1993;30(2):263–72.
[20] Chaudhuri RZ, Kabir HRH. Sensitivity of the response of moderately thick cross-ply doubly-curved panels to lamination and boundary constraint – ii. Application. Int J Solids Struct 1993;30(2):273–86.
[21] Chaudhuri RZ, Kabir HRH. Static and dynamic fourier analysis of finite cross-ply doubly curved panels using classical shallow shell theories. Compos Struct 1994;28(1):73–91.
[22] Oktem AS, Chaudhuri RZ. Levy type fourier analysis of thick cross-ply doubly curved panels. Compos Struct 2007;80(4):475–88.
[23] Oktem AS, Chaudhuri RZ. Fourier analysis of thick cross-ply levy type clamped doubly-curved panels. Compos Struct 2007;80(4):489–503.
[24] Oktem AS, Chaudhuri RZ. Higher-order theory based boundary-discontinuous fourier analysis of simply supported thick cross-ply doubly curved panels. Compos Struct 2009;89(3):448–58.
[25] Carrera E, Giunta G. Exact, hierarchical solutions for localised loadings in isotropic, laminated and sandwich shells. J Press Vess Technol 2009;131(4):041202.
[26] Carrera E. Theories and finite elements for multilayered plates and shells: a unified compact formulation with numerical assessment and benchmarking. Arch Comput Methods Eng 2003;10(3):215–96.
[27] Carrera E, Giunta G, Brischetto S. Hierarchical closed form solutions for plates bent by localized transverse loadings. J Zhejiang University Sci A 2007;8(7):1026–37.
[28] Carrera E, Giunta G. Hierarchical models for failure analysis of plates bent by distributed and localized transverse loadings. J Zhejiang University Sci A 2008;9(5):600–13.
[29] Carrera E, Giunta G. Hierarchical evaluation of failure parameters in composite plates. AIAA J 2009;47(3):692–702.
[30] Carrera E. Multilayered shell theories accounting for layerwise mixed description, part 1: governing equations. AIAA J 1999;37(9):1107–16.
[31] Carrera E. Multilayered shell theories accounting for layerwise mixed description, part 2: numerical evaluations. AIAA J 1999;37(9):1117–24.
[32] Carrera E. A priori vs. a posteriori evaluation of transverse stresses in multilayered orthotropic plates. Compos Struct 2000;48:245–60.
[33] Carrera E, Brischetto S. Analysis of thickness locking in classical, refined and mixed multilayered plate theories. Compos Struct 2008;82(4):549–62.
[34] Carrera E, Brischetto S. Analysis of thickness locking in classical, refined and mixed theories for layered shells. Compos Struct 2008;85(1):83–90.
[35] Koiter WT. A consistent first approximation in the general theory of thin elastic shells. In: Proc of symp. on the theory of thin elastic shells 1959;12–23.
[36] Murakami M. Laminated composites plate theory with improved in-plane responses. J Appl Mech 1986;53:661–6.
[37] Carrera E. On the use of murakami's zig–zag function in the modeling of layered plates and shells. Comput Struct 2004;82(7-8):541–54.
[38] Carrera E. Historical review of zig–zag theories for multilayered plates and shells. Appl Mech Rev 2003;56(3):287–308.
[39] Reddy JN. Mechanics of laminated composite plates and shells. Theory and Analysis. 2 ed. CRC Press; 2004.
[40] Reissner E. On a certain mixed variational theorem and a proposed application. Int J Numer Methods Eng 1984;20:1366–8.
[41] Reissner E. On a mixed variational theorem and on shear deformable plate theory. Int J Numer Methods Eng 1986;23:193–8.
[42] Federer H. The gauss–green theorem. Trans Am Math Soc 1945;58(1):44–76.
[43] Pagano NJ. Exact solutions for rectangular bidirectional composites and sandwich plates. J Compos Mater 1970;4:20–34.
[44] Sanders JL. Non-linear theories for thin shells. Quart Appl Math 1963;21:21–36.